FACTA UNIVERSITATIS
Series: **Mechanical Engineering**
https://doi.org/10.22190/FUME220806042S

Original scientific paper

FREE VIBRATION INVESTIGATION ON RVE OF PROPOSED HONEYCOMB SANDWICH BEAM AND MATERIAL SELECTION OPTIMIZATION

Babak Safaei[1,2], Emmanuel Chukwueloka Onyibo[1], Mehmet Goren[1], Kamila Kotrasova[3], Zhicheng Yang[4], Samaneh Arman[5], Mohammed Asmael[1]

[1]Department of Mechanical Engineering, Eastern Mediterranean University, Famagusta, Turkey
[2]Department of Mechanical Engineering Science,
University of Johannesburg, Gauteng, South Africa
[3]Department of Structural Mechanics, Institute of Structural Engineering,
Faculty of Civil Engineering, Technical University of Kosice, Slovakia
[4]College of Urban and Rural Construction,
Zhongkai University of Agriculture and Engineering, Guangzhou, China
[5]School of Science and Technology, University of Georgia, Tbilisi, Georgia

Abstract. *In this paper, free vibration, modal and stress state analyses of honeycomb sandwich structures with different boundary conditions was investigated and major factors affecting the sandwich frequencies and stiffness due to material or parameter changes were determined. The representative volume element (RVE) method used in this work were analytically and numerically validated by comparing the obtained results to those available in literature. Firstly, unit cell method was used to capture the entire effects of different parameters on the free vibration of honeycomb sandwich structure in ANSYS. This study analyzed the natural frequencies of honeycomb sandwich structures with different core materials combination. The effects of foil thickness, boundary conditions, materials selection, density and presence of crack on sandwich structure were taken into consideration and examined. The proposed core had an inbuilt shaped reinforcement with different materials for effective resonance, fatigue and deformation resistance at much higher frequency.*

Key words: *Honeycomb Sandwich Beam; Free vibration; Representative volume element; Mechanical properties*

Received August 06, 2022 / Accepted October 25, 2022
Corresponding author: Babak Safaei
Department of Mechanical Engineering, Eastern Mediterranean University, Famagusta, North Cyprus via Mersin 10, Turkey
Department of Mechanical Engineering Science, University of Johannesburg, Gauteng 2006, South Africa
E-mail: babak.safaei@emu.edu.tr

1. INTRODUCTION

Sandwich materials are becoming increasingly used in industry, particularly in the fields of transportation (automotive, aeronautics, shipbuilding, and railroads) and civil engineering [1]. In comparison to other panels, honeycomb panels provide high strength-to-weight ratios and design versatility [2]. Sandwich structures are often made up of two thin but strong face sheets and a low-density core [3,4]. Expansion method is generally used to create honeycomb for high density honeycomb materials [5], corrugated method is most commonly used as core [6]. In general, using theoretical computation and experimental methods, a number of studies have shown that constituent material, geometrical factors, and core cell topology have significant impacts on the mechanical performance of sandwich structures [7–9]. Circular honeycomb structures are supplementing, complementing, and supplanting traditional honeycomb structures. The application of these impact attenuation systems has become very popular among researchers.

Honeycombs are often made up of hexagonal or square cells [10–12] with the prismatic direction perpendicular to the plane of the sandwich panel's face plates. Styrene acrylonitrile (SAN) foam is a structural closed-cell thermoplastic core material with high toughness and impact resistance. Due to their chemical stability and high heat resistance, SAN foam cores can be used in demanding applications such as the production of cored prepreg laminates that need to withstand the heat and pressure of autoclave processing. Several core geometries and materials have been experimented by many researchers [13–20]. Furthermore, lightweight structures continue to advance as base materials. In addition, sandwich structures have fewer lateral deformations, higher buckling resistance, and higher natural frequencies than other structure types. Due to the appealing combination of light weight and strong mechanical properties, sandwich structures are commonly used in many manufacturing applications. Skins and their distance from the middle surface of composite affect tensile properties and especially flexural rigidity [21]. Therefore, in sandwich structures, steel is commonly applied for skins and cores can be made of almost any material [22,23]. The core material of sandwich structures is mostly a homogeneous and isotropic foam, which contributes to the sandwich's intense lightness. The materials commonly used in the core are metallic foams, polymers [24,25] and metals [26]. The behavior of nap-core sandwiches was investigated by Ha et al. [27] with special focus on the effect of symmetry. Onyibo and Safaei [28] applied finite element analysis to honeycomb sandwich structures. Mechanical properties and energy absorption capability of aluminum honeycomb structures were found to change with impact velocity [29]. However, honeycomb core is known for its great stiffness. Ha et al. [30] investigated the sensitivity of a nap-core sandwich, a unique type of structural composite. Chemami et al. [31] added orthogrid to improve the stiffness of soft honeycombs and thereby reduce interfacial mismatch in sandwich structures. Faria et al. [32] investigated the dynamic behaviors of sandwich beams with honeycomb cores loaded with magnetorheological (MR) gels and composite material skins under vibration. Hence, static deflection, frequency, and transient responses of the multilayer sandwich shell (flat/curved) structures under various forms of mechanical loads were estimated by Katariya and Panda [33]. Fazilati et al. [34] showed that honeycomb structures were commonly used as energy shock absorbers due to their strong crashworthiness characteristics of high energy absorption potential and high strength-to-weight ratio. Rama et al. [35,36] presented a linear triangular

shell element based on equivalent single-layer technique and an effective modeling tool for structures made of fiber-reinforced composite laminates with piezoelectric layers.

Unwanted structural vibrations can readily impact flexible structures, causing major issues such as structural instability, fatigue, and failure. Various research works have been conducted in order to avoid or control these vibratory disturbances in sandwich structures [37,38]. According to the law of vibration, everything (including components and structures) is in constant vibration at a given frequency. Zhao et al. [39] investigated the effect of nanotube aspect ratio on the free vibration characteristics of functionally graded nanocomposite cylinders reinforced with wavy single-walled carbon nanotubes (CNTs) using a mesh-free method. Moreover, a lot of frequency-based vibration on sandwich structures were investigated by many researchers [40–43] and as well as nonlinear bending/instability based vibration [44–49]. Liu et al. [50] examined the nonlinear forced vibrations of functionally graded materials (FGMs). Li et al. [51] theoretically and experimentally studied the nonlinear vibrations of fiber-reinforced composite cylindrical shells (FRCCSs) with bolted joint boundary conditions. Liu et al. [52] developed a novel method for solving nonlinear forced vibrations of functionally graded (FG) piezoelectric shells in multi-physics fields. Moradi-Dastjerdi and Behdinan [53] studied free vibration behaviors of a multifunctional smart sandwich plate (MSSP) using an advanced and reliable method. Hence, several current research are being carried out on nonlinear forced vibrations [54,55] and nonlinear dynamic responses [56–61] of FGM sandwich structures.

In this work, the dynamic behaviors of mechanical structures, particularly composite structures, are well recognized to be crucial to the efficient functioning of a variety of applications, including automotive, civil, and aeronautic sectors. Failure may be prevented by understanding practical structural behaviors and unwanted resonance can be minimized or decreased. In general, an overall understanding of modal analysis and natural frequencies for honeycomb sandwich beams with different material properties and boundary conditions are detailed while taking into account their density. Moreover, the proposed core orthotropic stiffness matrix is investigated. In general, an elliptical cut on sandwich beam at various positions is analyzed and natural frequency is observed.

2. Geometric Modelling of Honeycomb Sandwich Beam

The software ANSYS 21.R2 Spaceclaim was used to develop the finite element model of the honeycomb sandwich beam. The sandwich structure developed in this research had dimensions of 290 mm x 40 mm x 11 mm. The thicknesses of the honeycomb sandwich beam face-sheet and core were 1 and 9 mm, respectively. The geometries of hexagonal unit cell and proposed unit cell are depicted in Figs. 1(a) and (b). Moreover, the proposed structure was a honeycomb hexagonal structure with an inbuilt star shaped reinforcement. Hence, in order to investigate the natural frequencies of free vibrations with different boundary conditions, inbuilt star shaped cores made of different materials were analyzed. in addition, the considered factors were the mass and stiffness of the overall sandwich beam while considering vibration characteristics, corresponding natural frequencies and mode shapes. In general, RVE method in ANSYS Material Designer were used to determine effective elastic properties of hexagonal honeycomb and proposed core by capturing their unit cell. The Material Designer module is used to capture the domain of an entire honeycomb and proposed core structure, as it is expected that the unit cell was repeated

uniformly over the entire domain of the structure. Hence, the result was obtained as an orthotropic stiffness matrix, which could then be used as a material property in larger structures. Material properties required in this study are summarized in Table 1. In general, carbon fiber, SAN foam, aluminum alloy and polyvinyl chloride (PVC) foam materials were applied in finite element analysis. SAN foam has mechanical properties comparable to those of cross-linked PVC but has the toughness and elongation of uncross-linked PVCs.

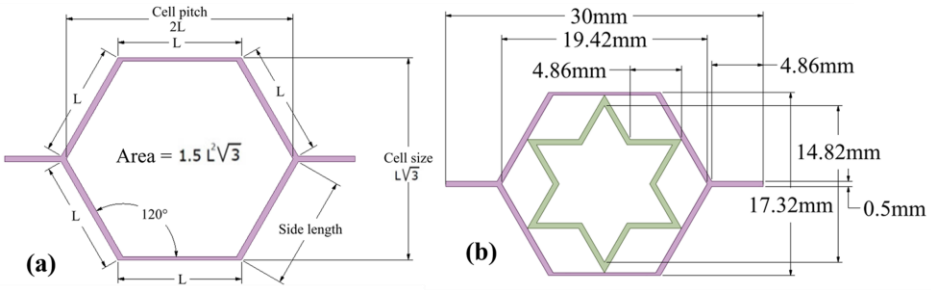

Fig. 1 Geometry of (a) Honeycomb unit cell and (b) Honeycomb with star shaped reinforced unit cell

Table 1 Material properties of honeycomb sandwich beams

Material	Young's Modulus E (MPa)	Poisson's Ratio ν	Shear Modulus G (MPa)	Density ρ (Kg/m^3)
Carbon fiber	290000	0.2	9000	1800
SAN Foam	85	0.3	32.69	103
Aluminum Alloy	71000	0.33	26691.72	2770
PVC Foam	102	0.3	39.23	80

2.1 Finite Element Meshing

In order to covert the geometry bodies to finite element entities for hexagonal and proposed core unit cell. Hence, 'Mesh' in RVE model group was selected with maximum mesh size of 0.25 mm (half the thickness of the unit cell), the periodic meshing and conformal meshing were used for both cores' unit cell, their number of elements and nodes are depicted in Table 2. Fig. 2 shows the equivalent models of regular hexagonal honeycomb and proposed reinforced star-shaped core. Hexagonal honeycombs are consisted of a 'unit cell' repeated many times along one or more spatial directions. This unit cell is usually a fraction of the size of the overall structure under investigation. Hence, in ANSYS Workbench 2021, a new feature called "Material Designer" was used for the homogenization of hexagonal and proposed core of the sandwich beam. Moreover, this technique equally reduced the computational time of the analysis. In general, the final result is an orthotropic stiffness matrix, which can subsequently be used as a material property in larger structures and honeycomb structure is replaced with 'homogenized' (effective) material properties shown in Table 3. Material Designer gives nine independent material

constants including three elastic moduli, three shear constants, and three Poisson ratios. A mesh sensitivity analysis was carried out in order to determine the mesh resolution required for accurate results. Furthermore, both models were run with various mesh sizes, the resulting stress or displacement values were observed. Thus, due to the addition of star geometry reinforcement, the proposed core unit cell has more nodes and elements than a normal hexagonal honeycomb. Therefore, there was 33.1% increase in the number of elements and 32.2% increase in the number of nodes in the proposed core model when compared with the traditional hexagonal honeycomb core shape. In addition to that, the computation time is almost the same with 3-5 second's difference in analysis time.

Table 2 Analysis mesh of both unit cell core

Unit cell	Number of Elements	Number of Nodes
Hexagonal honeycomb core	2210	4956
Proposed core	2942	6553

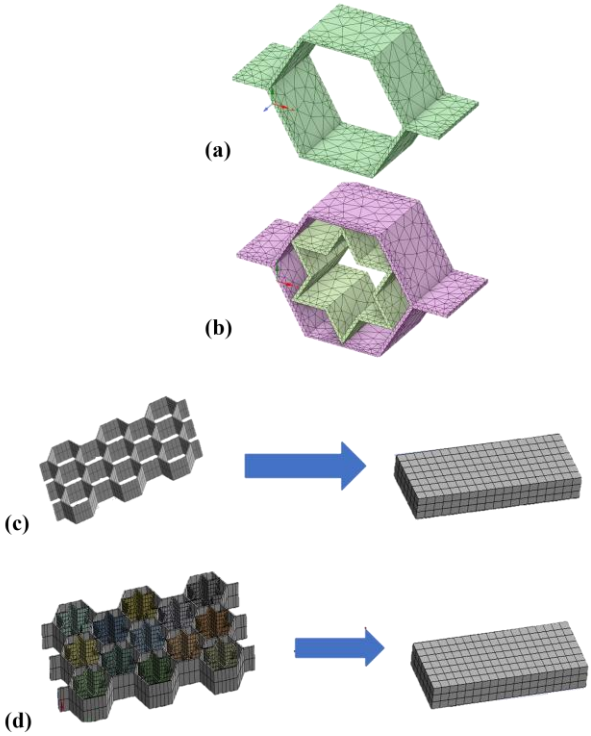

Fig. 2 Meshing of (a) hexagonal meshing; (b) proposed core meshing; (c) homogenized model of hexagonal core meshing; and (d) homogenized model of proposed core meshing

The RVE modeling of hexagonal honeycomb and proposed core were homogenized, geometries were simplified, and material properties of the constituent materials were defined. In general, geometry was meshed for finite element analysis.

Table 3 Orthotropic material properties of RVE proposed core

Material Hexagonal	Material Star core	Density (kg/m^3)	Ex = Ey (MPa)	Ez (MPa)	υxy	υyz = υxz (10^{-3})	Gx (MPa)	Gy = Gz (MPa)
SAN Foam	SAN Foam	11.29	0.1161	9.3191	0.957	3.7	0.01121	1.3762
SAN Foam	PVC	10.07	0.1315	10.215	0.951	3.8	0.01142	1.4188
SAN Foam	Aluminum Alloy	151.94	2.4994	3749.12	0.118	0.2	0.01580	1.8990
SAN Foam	Carbon Fiber	100.78	2.5332	1218.78	0.027	0.3	0.01578	1.8960
Single Hexagonal SAN Foam material		5.86	0.0278	4.84	0.988	1.7	0.00699	0.9548

2.2 Modelling boundary conditions

The boundary condition of the sandwich beam was chosen as clamped-free and clamped-clamped, as shown in Figs. 3(a) and 3(b), respectively, for free vibration analyses. Hence, for elliptical cut investigation, clamped-free boundary condition was considered, while elliptical cut position changed along the length of the beam, as shown in Fig. 3(c). Moreover, elliptical cut depth was throughout the sandwich beam with 30 mm in diameter. Table 4 depicts the dimensions of honeycomb sandwich beam.

Table 4 Dimensions of the honeycomb sandwich beam

Cell size (mm)	Core thickness (mm)	Cell thickness (mm)	skin (mm)	Length (mm)	Width (mm)
10	9	0.5	1	290	40

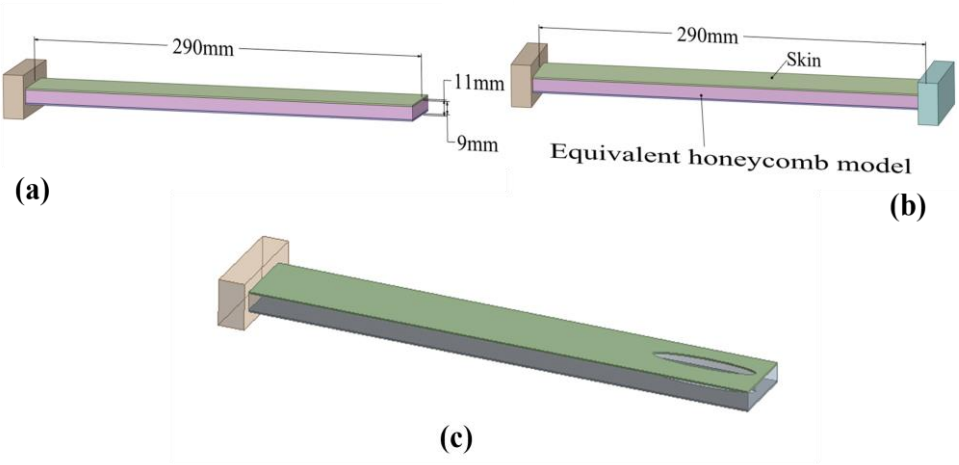

Fig. 3 Boundary conditions (a) Clamped-free; (b) Clamped-clamped; (c) Clamped-free with elliptical cut

3. FEM ANALYSIS

3.1 Analytical models

Beam theory [62,63] is commonly used to calculate in plane elastic characteristics of honeycombs, for which the radius of curvature in nodes is neglected (Fig. 4). The effective Young's moduli parallel to *OX* and *OY*, effective Poisson's ratios and effective shear modulus for commercial honeycomb, i.e. $t_1 = t$ and $t_2 = 2t$ could be evaluated taking into account bending stresses in cell walls, applicable for when $t << \ell$ [62,63]:

$$E_1 = E_s \left(\frac{t}{\ell}\right)^3 \frac{\cos\theta}{\left(\frac{h}{\ell}+\sin\theta\right)\sin^2\theta} \tag{1}$$

$$E_2 = E_s \left(\frac{t}{\ell}\right)^3 \frac{\frac{h}{\ell}+\sin\theta}{\cos^3\theta} \tag{2}$$

$$v_{12} = \frac{\cos^2\theta}{\left(\frac{h}{\ell}+\sin\theta\right)\sin\theta}; v_{21} = \frac{1}{v_{12}} \tag{3}$$

$$G_{12} = E_s \left(\frac{t}{\ell}\right)^3 \frac{\frac{h}{\ell}+\sin\theta}{\left(\frac{h}{\ell}\right)^2\left(1+\frac{h}{4\ell}\right)\cos\theta} \tag{4}$$

where E_1, and E_2 are effective Young's moduli of honeycomb core in the material system of coordinates, E_s is Young's modulus of solid cell wall material, v_{12} and v_{21} are effective Poisson's ratio of honeycomb core in the material and G_{12} is effective shear modulus.

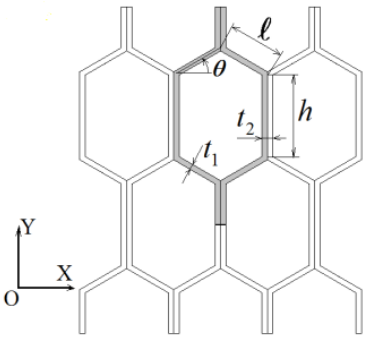

Fig. 4 Basic cell used in analytical calculus

3.2 Equivalent honeycomb sandwich beam

The created equivalent model was used in this research. Hence, the time spent for the analysis was reduced and computational time was decreases significantly. Homogenization concept is regularly used in the research on the mechanical behaviors of composite materials. This method allows for the avoidance of difficulties associated with heterogeneities. Therefore, the conceptualization of this method is basically by considering the genuine constitution of material/geometry arrangement and it is considered to be

continuous throughout the entire structure. However, “Material Designer” analysis system in ANSYS Workbench was used for this technique.

4. RESULTS AND DISCUSSIONS

4.1 Free vibration of honeycomb beam

In this section, a modal analysis of honeycomb equivalent sandwich beam was presented. The numerically and analytically results obtained in this study were compared with experimental data from the available literature. The honeycomb structures will be parameterized in order to get insight on factors that can affect it natural frequencies by considering the effect of boundary conditions, foil thickness and materials. In general, the proposed reinforced star core was introduced and examined. Consequently, density was considered. Furthermore, the best material combination for high flexural stiffness, higher frequency and lighter weight was investigated for the proposed core structure. Considering a classical honeycomb with an isotropic material having E_s = 1000 MPa, ρ = 1000 kg/m^3 v_s = 0.3, t = 1 mm and L = 10 mm, the analytically obtained results (Eqs. 1-4) along with those of FEM are presented in Table 5. However, having validated the regular honeycomb RVE with the available literature using ANSYS Material Designer analysis system. Moreover, the same analysis system was used for the proposed core model unit cell and its orthotropic material properties were equally obtained.

Table 5 Results for the validation of RVE models

Regular honeycomb: L= h =10 mm and θ = 30º						
Model	ρ (kg/m^3)	E_1 (MPa)	E_2 (MPa)	G_{12} (MPa)	V_{12}	V_{21}
Analytic	115.5	2.18	2.18	0.56	0.96	0.96
Present	112.14	2.572	2.572	0.657	0.957	0.957
Solid 3D [64]	112.10	2.570	2.570	0.660	0.960	0.960

4.2 Effects of materials on free vibration

Under modal analysis, the natural frequencies of sandwich beams with deferent materials were investigated and their corresponding deformations were noted. Howover, considering the effect of free vibration of honeycomb core, Fig. 5 shows a hexagonal honeycomb core (HC) with the same dimensions having cantilever beam boundary conditions, simulated with three different materials of aluminum alloy, carbon fiber and SAN foam in order to investigate their natural frequencies and mode shapes. It was observed that aluminum had much higher natural frequency, followed by carbon fiber and SAN foam had the lowest natural frequency. As a result of that, aluminum alloy is stiffer than the rest, especially those subjected to double tension and compression cyclic loading. Moreover, while considering sandwich structure deformation in line with their corresponding frequencies, Fig. 6 depicts the deformation of three sandwich core materials on free vibration analysis. As expected, SAN foam with the lowest natural frequency tends to vibrate more at any slightest excitation, as result of that it had the highest amount of

deformation when compared with the rest materials. It was observed that carbon fiber had the lowest deformation, indicating that carbon fiber has higher stiffness to mass ratio than aluminum alloy.

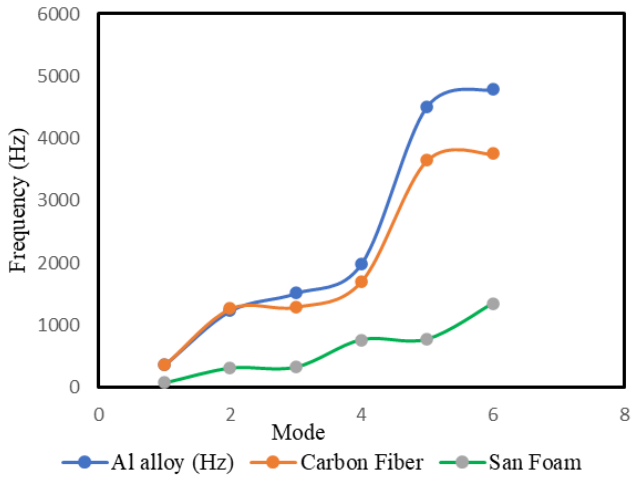

Fig. 5 Effects of materials on natural frequency

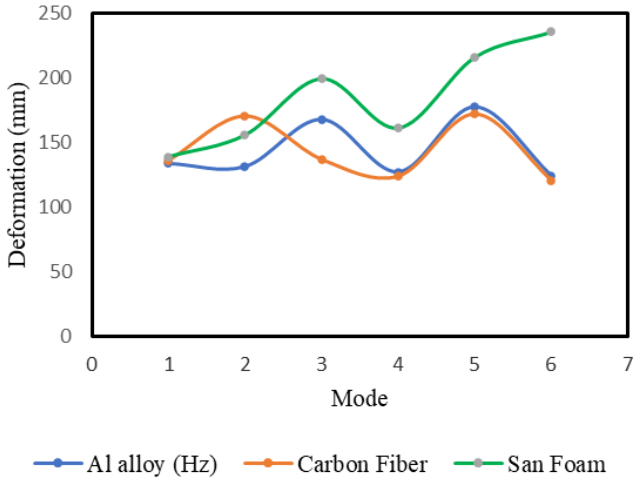

Fig. 6 Effects of materials on deformation

4.3 Effect of Boundary Conditions (CF and CC) on the Free Vibration of Sandwich structure

Considering the effect of boundary conditions on sandwich beam structure. In this section, clamped-free and clamped-clamped boundary condition was applied on sandwich beam while their vibrational response is observed. Fig. 7 shows mode 5 directional deformation of the sandwich structure under clamped-free condition with 3 different

materials used as core. However, carbon fiber and aluminum core had similar deformation patterns while SAN foam deviated much with multiple tension and compressive stresses due to lower flexural stiffness. Moreover, in order to get insight on sandwich structure and monitor incremental changes, clamp-clamp boundary condition was investigated, as shown in Fig. 8. It was observed that the peak amplitude of SAN foam sandwich core was higher, which resulted in larger deformation and underwent 4 tensile and compressive stresses. In general, fixed-fixed boundary conditions increased sandwich beam natural frequency as well as corresponding directional deformation.

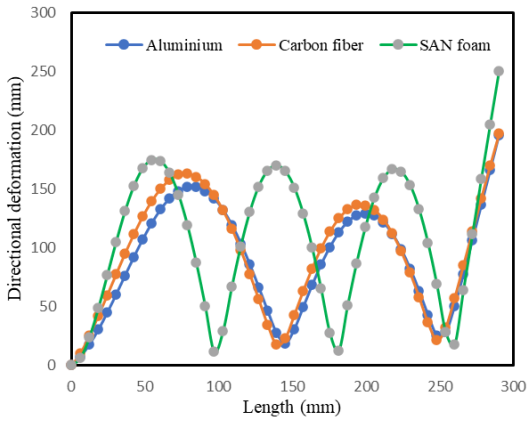

Fig. 7 Directional deformation on Mode 5 (Clamped-free)

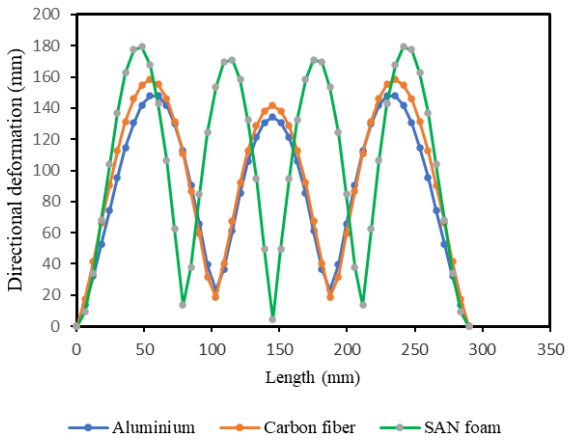

Fig. 8 Directional deformation on Mode 5 (Clamped-clamped)

4.4 Effect of hexagonal cell foil thickness on free vibration

In this case, the effect of the parameters of hexagonal cell on free vibration were investigated. Hence, sandwich structure dimensions including sandwich length and thickness were kept the same and cell dimension were changed. Fig. 9 shows the free vibration of foil thickness (FT). It was observed that as the foil thickness was increased,

natural frequency was decreased under clamped-free boundary condition. In addition, variations were close and almost negligible, indicating that changing foil thickness did not significantly affect the vibration characteristics of honeycomb sandwich structures and only the weight of the structure was increased, as shown in Table 6, such that 10% increase of foil thickness increases density by about 9%. Furthermore, when foil thickness was increased, Young's modulus was increased such that increase of foil thickness by 10% increased elasticity modulus by 32.7%. Further increase of thickness also increased elasticity modulus but in lower rates. Therefore, when foil thickness was increased by 7% (from 1.4 to 1.5mm) Young's modulus was increased by 21.7%.

Table 6 Variation of density and foil thickness

Foil Thickness	Thickness	Density (kg/m^3)	E_x (MPa)	E_y (MPa)	υxy	G_x (MPa)
1	10	385.39	403.95	403.95	0.92	104.18
1.1	10	422.34	536.20	536.20	0.91	138.88
1.2	10	459.00	689.35	689.35	0.89	180.20
1.3	10	495.38	859.31	859.31	0.88	227.69
1.4	10	531.46	1070.68	1070.68	0.86	284.47
1.5	10	567.26	1303.13	1303.13	0.84	346.21

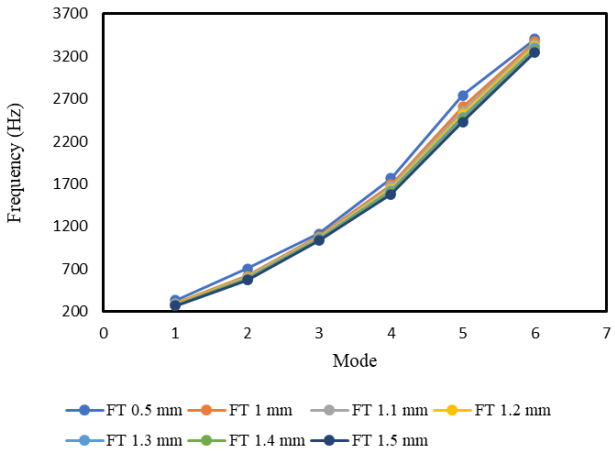

Fig. 9 Variation of frequency with respect to foil thickness

4.5 Prestressed Modal Analysis of Sandwich Structure

Investigating prestressed modal analysis and how the mode frequencies of the sandwich beams changes with thermal load at different values. Hence, in order to generate thermal stresses, the sandwich beam was constrained at both ends and was kept at room

temperature. Moreover, the total strain developed was equal to the sum of elastic and thermal strains. In this case, since the sandwich was fully constrained along axial direction, total strain was zero in all cases and therefore, the elastic strain developed in the sandwich was equal in magnitude but opposite in sign compared to thermal strain. Therefore, when thermal load was higher than reference temperature, thermal strain was positive and this made the elastic strain negative which indicated compressive stresses on sandwich beam. Similarly, when thermal load on sandwich beam was less than reference temperature, thermal strain was negative. Therefore, elastic strain was positive and tensile stresses were developed in the sandwich beam. Fig. 10 depicts the changes of mode frequencies with thermal loads.

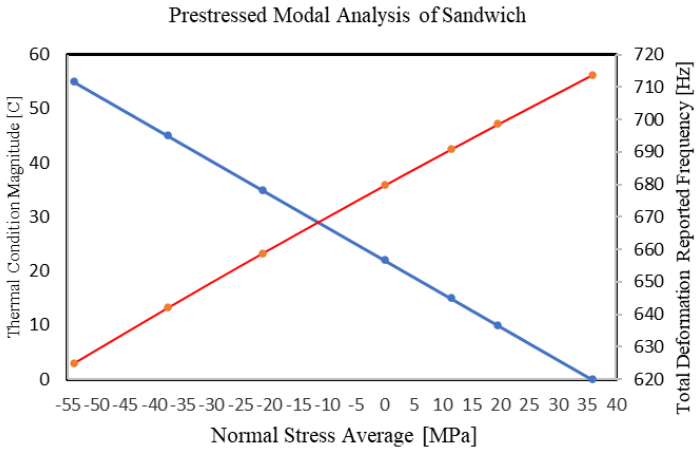

Fig. 10 Frequency changes with thermal load

4.6 Proposed reinforced star core model

Hexagonal honeycomb was further designed to accommodate star shaped core in the center. However, central core provided excellent torsional resistance while hexagonal-shaped one provided extremely lateral bending resistance. Hence, a simulation was carried out in ANSYS Workbench, whereby different materials were assigned to the proposed model. In this case, SAN foam was remained as regular hexagonal material while the star shaped reinforcing materials varied to SAN foam, PVC foam, aluminum alloy and carbon fiber, as shown in Fig. 11. Table 7 summarizes the natural frequency of the proposed core under clamped-clamped boundary condition with different material combinations. Fig. 12 shows the natural frequency of the proposed core model under clamped-clamped boundary conditions. It was observed that the cores with hexagonal SAN foam and PVC foam star shaped reinforcements had higher stiffness to mass ratios and natural frequencies than remaining structures. Moreover, repeating the same simulation of the proposed core natural frequency under clamped-free condition, PVC and SAN foams still presented the best material combination for higher frequencies, as shown in Fig. 13.

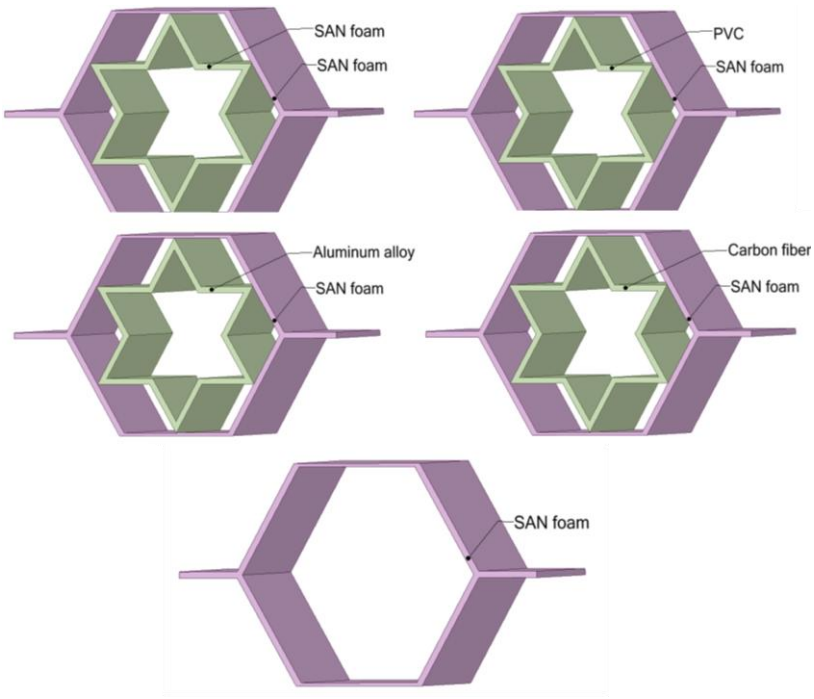

Fig. 11 Proposed core material selections

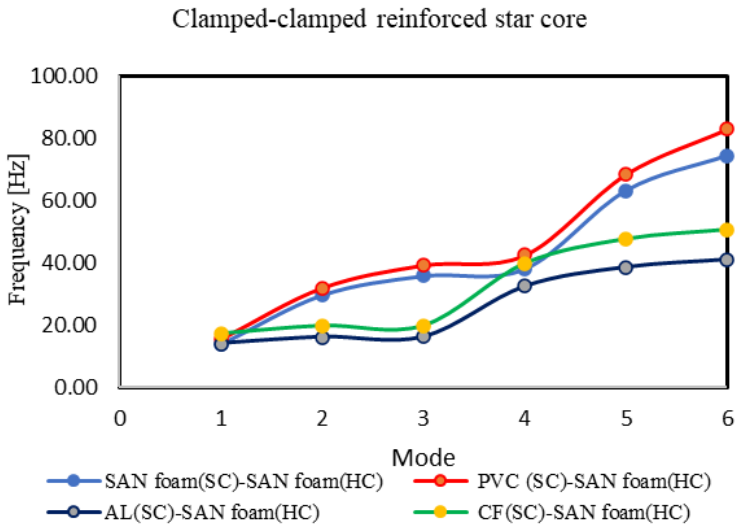

Fig. 12 Natural frequency of the proposed core (Clamped-clamped)

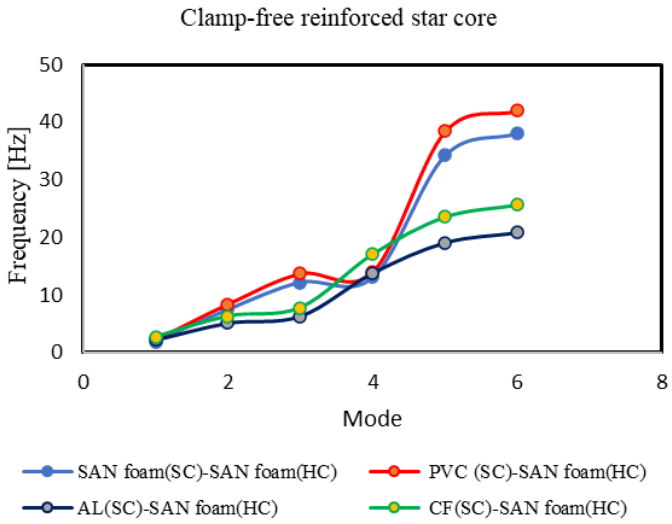

Fig. 13 Natural frequency of the proposed core (Clamped-free)

Table 7 Natural frequency of the free vibration response of the proposed reinforced star core model under clamped-clamped boundary condition

Mode	SAN foam (SC)- SAN foam (HC) (Hz)	PVC (SC)- SAN foam (HC) (Hz)	AL(SC)- SAN foam (HC) (Hz)	CF(SC)- SAN foam (HC) (Hz)	SAN foam HC shape only (Hz)
1	13.87	15.48	14.08	17.38	11.16
2	29.67	31.95	16.14	19.88	31.1
3	35.82	39.24	16.19	19.9	31.67
4	38.07	42.45	32.43	39.83	33.31
5	63.18	68.37	38.6	47.66	61.92
6	74.43	82.89	41.07	50.67	68.82
Density kg/m^3	512.88	511.88	627.95	586.1	508.39

4.6.1 Comparison of flexural stiffness of the proposed core

In order to investigate the deformation resistance of the proposed core, the reinforcement was assigned different materials. The applied force was 100 N which was kept constant for all material combinations. Hexagonal shape material was kept constant and only star shaped reinforcement material was changed. The obtained results are summarized in Table 8. In line with the obtained results, it was observed that the stresses were almost constant since they were irrespective of rigidity modulus. Also, all proposed

cores had the same shape, cross-section area and applied load. However, there were significant changes in their deflection, due to material combination stiffness, in which SAN foam and carbon fiber showed the highest deformation resistance.

Table 8 Comparison of material stiffness in the proposed cores

	SAN foam (SC)- SAN foam (HC)	PVC (SC)- SAN foam (HC)	AL(SC)- SAN foam (HC)	CF(SC)- SAN foam (HC)
Equivalent Stress Maximum [MPa]	6.76	6.76	6.72	6.71
Total Deformation Maximum [mm]	113683.82	100417.08	5250.74	5173.66

4.7 Elliptical cut on sandwich beam

Effect of elliptical cut on sandwich beam natural frequency was studied. The sandwich beam has an elliptical cut of 30 mm throughout its layers. Hence, fixed-free boundary condition was used for the modal analysis of sandwich beam with elliptical cut. The analysis on sandwich beam was carried out in ANSYS software. However, it was observed that cut on sandwich might increase or reduce its free vibration characteristics, depending on the size, position, shape and depth of the cut. Hence, in this case, elliptical shape cut throughout the thickness of the sandwich was considered. Therefore, it was observed that as the elliptical cut moved closer to the fixed support, natural frequency was reduced. In addition, the sandwich with elliptical cut was compared with normal sandwich beam with no cut. However, when the cut was 255 mm away from the fixed support, natural frequency became higher than that of normal sandwich beam without cut. In general, aluminum alloy material was used as core and skin. Also, regular hexagonal honeycomb shape was used as core. Fig. 14 shows the position of elliptical cut at 6 different distances along the length of the sandwich beam towards the fixed support, illustrating that when the elliptical cut came closer to fixed support, sandwich natural frequency was reduced. The first 3 mode shapes of normal and damaged sandwich beams are depicted in Figs. 15 and 16, respectively.

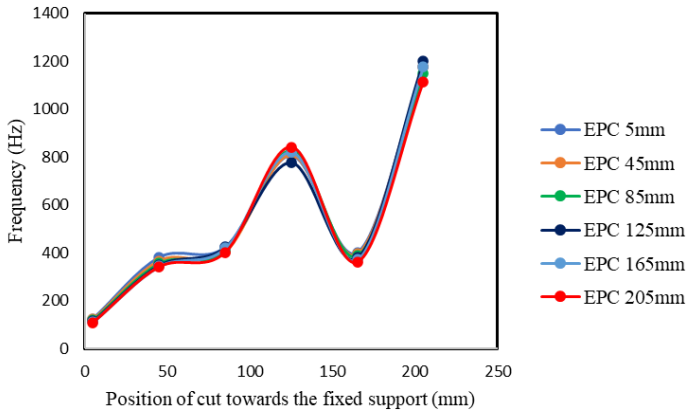

Fig. 14 Positions of elliptical cut vs natural frequency

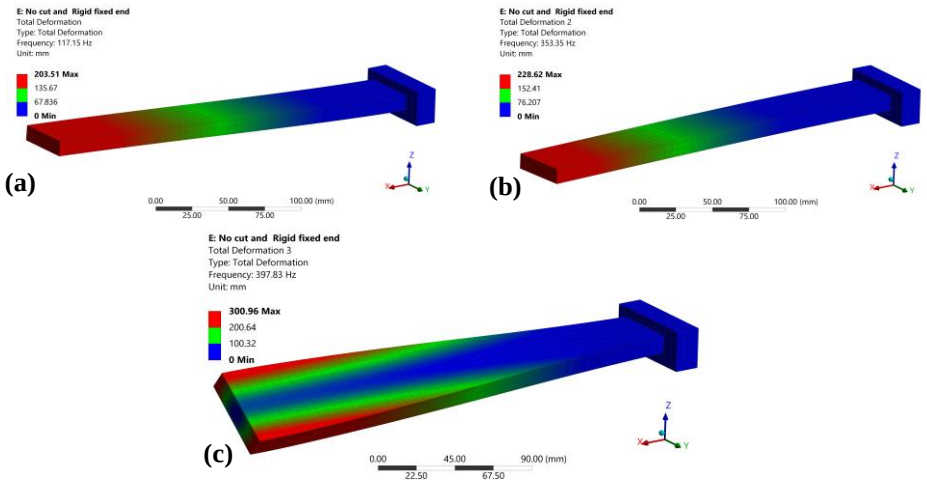

Fig. 15 First 3 mode shape contours of sandwich beam (a) Mode 1 total deformation 203.51 mm, 117.15 Hz (bending); (b) Mode 2 total deformation 228.62 mm, 353.35 Hz (bending); (c) Mode 3 total deformation 300.96 mm, 397.83 Hz (torsion)

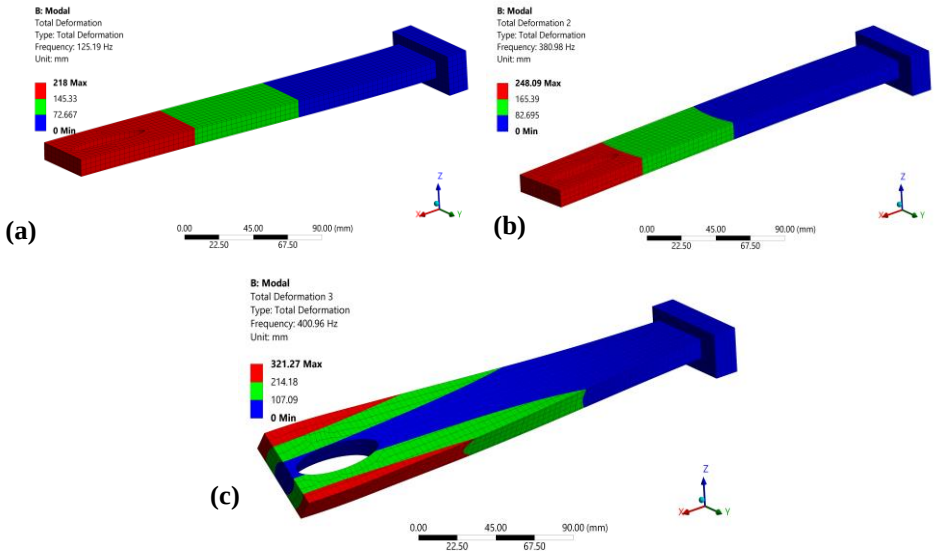

Fig. 16 First 3 mode shape contours of sandwich beam with elliptical cut (a) Mode 1 total deformation 218 mm, 125.19 Hz (bending); (b) Mode 2 total deformation 248.09 mm, 380.98 Hz (bending); (c) Mode 3 total deformation 321.27 mm, 400.96 Hz (torsion)

5. CONCLUSIONS

The results of a detailed honeycomb sandwich beam modal analysis and simulation were shown and plotted, and significant observations were recorded. The free vibration of a honeycomb sandwich beam was examined and validated using available literature and the model was developed using ANSYS software. However, the validity of the model developed in this study for the computation of in-plane mechanical properties was confirmed by the results of hexagonal RVE numerical investigations using ANSYS Material Designer.

Vibrational behavior of honeycomb sandwich beam was affected by many factors as witnessed in parametric analysis results. Hence, natural frequency was changed by geometry, material, presence of crack or cut, induced thermal load and boundary conditions. Natural frequency was also a function of stiffness to mass ratio. The proposed model was designed to have reinforced inbuilt star shape core which enhanced vibration characteristics, it was further optimized by changing star shaped reinforcement materials. Therefore, the material SAN foam hexagonal and PVC foam star core (SC) reinforcement had higher stiffness to mass ratios and natural frequencies. In addition, increasing foil thickness did not have significant effect on sandwich beam natural frequency but increased the weight and Young's modulus of the structure. In general, presence of a cut in a sandwich beam affects its natural frequency such that the frequency was reduced in under fixed-fixed boundary condition, while under fixed-free boundary condition, it depends on the size, depth and position of the cut. In this experiment, 30 mm elliptical cut throughout the sandwich beam 255 mm away from the fixed support increased natural frequency while for elliptical cut of 55 mm away from the fixed-free boundary support, natural frequency was reduced as compared with non-damaged sandwich beam. In general, it was observed that the proposed core structure has better vibrational response than the hexagonal honeycomb model, and assigning different materials for the star shape reinforcement further improves the stiffness and increased natural frequencies of the structure. In the other hands, instead of increasing core thickness to achieve greater stiffness as a way of increasing the area moment of inertia, the proposed core should be used and good materials for the reinforcement should equally be considered based on the design criteria.

REFERENCES

1. Manet, V., 1998, *The use of ANSYS to calculate the behaviour of sandwich structures*, Composites Science and Technology, 58(12), pp. 1899–1905.
2. Satya Krishna, P., Mohan Vemula, A., Umar Ahamed, P., Jani, S.P., 2022, *Bending analysis of honeycomb sandwich panels with metallic face sheets and GFRP core*, Materials Today: Proceedings, 60, pp. 1537–1547.
3. Sayyad, A.S., Ghugal, Y.M., 2015, *On the free vibration analysis of laminated composite and sandwich plates: A review of recent literature with some numerical results*, Composite Structures, 129, pp. 177–201.
4. Stocchi, A., Colabella, L., Cisilino, A., Álvarez, V., 2014, *Manufacturing and testing of a sandwich panel honeycomb core reinforced with natural-fiber fabrics*, Materials and Design, 55, pp. 394–403.
5. Zhang, Z., Wei, X., Wu, K., Wang, Y., Jia, Z., Zhang, Q., Jin, F., 2022, *Failure analysis of brazed sandwich structures with square honeycomb-corrugation hybrid cores under three-point bending*, Thin-Walled Structures, 170, 108591
6. Kang, R., Shen, C., Lu, T.J., 2022, *A three-dimensional theoretical model of free vibration for multifunctional sandwich plates with honeycomb-corrugated hybrid cores*, Composite Structures, 298, 115990.

7. Sun, G., Zhang, J., Li, S., Fang, J., Wang, E., Li, Q., 2019, *Dynamic response of sandwich panel with hierarchical honeycomb cores subject to blast loading*, Thin-Walled Structures, 142, pp. 499–515.
8. Sun, M., Wowk, D., Mechefske, C., Kim, I.Y., 2019, *An analytical study of the plasticity of sandwich honeycomb panels subjected to low-velocity impact*, Composites Part B: Engineering, 168, pp. 121–128.
9. Liu, Y., Qin, Z., Chu, F., 2022, *Analytical study of the impact response of shear deformable sandwich cylindrical shell with a functionally graded porous core*, Mechanics of Advanced Materials and Structures, 29(9), pp. 1338–1347.
10. Zhu, R., Zhang, X., Zhang, S., Dai, Q., Qin, Z., Chu, F., 2022, *Modeling and topology optimization of cylindrical shells with partial CLD treatment*, International Journal of Mechanical Sciences, 220, 107145
11. Wei, X., Li, D., Xiong, J., 2019, *Fabrication and mechanical behaviors of an all-composite sandwich structure with a hexagon honeycomb core based on the tailor-folding approach*, Composites Science and Technology, 184, 107878.
12. Wang, R., Wang, J., 2018, *Modeling of honeycombs with laminated composite cell walls*, Composite Structures, 184, pp. 191–197.
13. Liu, Y., Qin, Z., Chu, F., 2021, *Nonlinear dynamic responses of sandwich functionally graded porous cylindrical shells embedded in elastic media under 1: 1 internal resonance*, Applied Mathematics and Mechanics, 42(6), pp. 805–818.
14. Wang, Z., 2019, *Recent advances in novel metallic honeycomb structure*, Composites Part B: Engineering, 166, pp. 731–741.
15. Feng, G., Li, S., Xiao, L., Song, W., 2021, *Energy absorption performance of honeycombs with curved cell walls under quasi-static compression*, International Journal of Mechanical Sciences, 210, 106746.
16. D'Mello, R.J., Waas, A.M., 2013, *Inplane crush response and energy absorption of circular cell honeycomb filled with elastomer*, Composite Structures, 106, pp. 491–501.
17. Birman, V., Kardomateas, G.A., 2018, *Review of current trends in research and applications of sandwich structures*, Composites Part B: Engineering, 142, pp. 221–240.
18. Safaei, B., Onyibo, E.C., Hurdoganoglu, D., 2022, E*ffect of static and harmonic loading on the honeycomb sandwich beam by using finite element method*, Facta Universitatis, Series: Mechanical Engineering, doi: 10.22190/FUME220201009S
19. Barbaros, I., Yang, Y., Safaei, B., Yang, Z., Qin, Z., Asmael, M., 2022, *State-of-the-art review of fabrication, application, and mechanical properties of functionally graded porous nanocomposite materials*, Nanotechnology Reviews, 11(1), pp. 321–371.
20. Safaei, B., Onyibo, E.C., Hurdoganoglu, D., *Thermal buckling and bending analyses of carbon foam beams sandwiched by composite faces under axial compression*, Facta Universitatis, Series: Mechanical Engineering, doi:10.22190/FUME220404027S
21. Douville, M.A., Le Grognec, P., 2013, *Exact analytical solutions for the local and global buckling of sandwich beam-columns under various loadings*, International Journal of Solids and Structures, 50(16–17), pp. 2597–2609.
22. Zhang, F., Liu, W., Ling, Z., Fang, H., Jin, D., 2018, *Mechanical performance of GFRP-profiled steel sheeting composite sandwich beams in four-point bending*, Composite Structures, 206, pp. 921–932.
23. Sohel, K.M.A., Richard Liew, J.Y., 2011, *Steel–Concrete–Steel sandwich slabs with lightweight core — Static performance*, Engineering Structures, 33(3), pp. 981–992.
24. Reyes, G., 2008, *Static and low velocity impact behavior of composite sandwich panels with an aluminum foam core*, Journal of Composite Materials, 42(16), pp. 1659–1670.
25. Mamalis, A.G., Spentzas, K.N., Manolakos, D.E., Ioannidis, M.B., Papapostolou, D.P., 2008, *Experimental investigation of the collapse modes and the main crushing characteristics of composite sandwich panels subjected to flexural loading*, International Journal of Crashworthiness, 13(4), pp. 349–362.
26. Crupi, V., Epasto, G., Guglielmino, E., 2012, *Collapse modes in aluminium honeycomb sandwich panels under bending and impact loading*, International Journal of Impact Engineering, 43, pp. 6–15.
27. Ha, G.X., Zehn, M.W., Marinkovic, D., Fragassa, C., 2019, *Dealing with Nap-Core Sandwich Composites: How to Predict the Effect of Symmetry*, Materials, 12(6), 874.
28. Onyibo, E.C., Safaei, B., 2022, *Application of finite element analysis to honeycomb sandwich structures: a review*, Reports in Mechanical Engineering, 3(1), pp. 283–300.
29. Wang, Z., Tian, H., Lu, Z., Zhou, W., 2014, *High-speed axial impact of aluminum honeycomb - Experiments and simulations*, Composites Part B: Engineering, 56, pp. 1–8.
30. Ha, G.X., Marinkovic, D., Zehn, M.W., 2019, *Parametric investigations of mechanical properties of nap-core sandwich composites*, Composites Part B: Engineering, 161, pp. 427–438.
31. Chemami, A., Bey, K., Gilgert, J., Azari, Z., 2012, *Behaviour of composite sandwich foam-laminated glass/epoxy under solicitation static and fatigue*, Composites Part B: Engineering, 43(3), pp. 1178–1184.

32. Faria, L.E.R., Gomes, G.F., de Sousa, S.R.G., Bombard, A.J.F., Ancelotti Jr, A.C., 2020, *Dynamic experimental behavior of sandwich beams with honeycomb core filled with magnetic rheological gel: a statistical approach*, Smart Materials and Structures, 29(11), 115044.
33. Katariya, P. V., Panda, S.K., 2019, *Numerical evaluation of transient deflection and frequency responses of sandwich shell structure using higher order theory and different mechanical loadings*, Engineering with Computers, 35(3), pp. 1009–1026.
34. Fazilati, J., Alisadeghi, M., 2016, *Multiobjective crashworthiness optimization of multi-layer honeycomb energy absorber panels under axial impact*, Thin-Walled Structures, 107, pp. 197–206.
35. Rama, G., Marinkovic, D., Zehn, M., 2018, *High performance 3-node shell element for linear and geometrically nonlinear analysis of composite laminates*, Composites Part B: Engineering, 151, pp. 118–126.
36. Rama, G., Marinković, D., Zehn, M., 2017, *Efficient three-node finite shell element for linear and geometrically nonlinear analyses of piezoelectric laminated structures*, Journal of Intelligent Material Systems and Structures, 29(3), pp. 345–357.
37. Sahu, S.K., Badgayan, N.D., Samanta, S., Sahu, D., Sreekanth, P.S.R., 2018, *Influence of cell size on out of plane stiffness and in-plane compliance character of the sandwich beam made with tunable PCTPE nylon honeycomb core and hybrid polymer nanocomposite skin*, International Journal of Mechanical Sciences, 148, pp. 284–292.
38. Peng, X.L., Bargmann, S., 2021, *A novel hybrid-honeycomb structure: Enhanced stiffness, tunable auxeticity and negative thermal expansion*, International Journal of Mechanical Sciences, 190, 106021.
39. Zhao, Z., Safaei, B., Wang, Y., Liu, Y., Chu, F., Wei, Y., 2022, *Atomistic scale behaviors of intergranular crack propagation along twist grain boundary in iron under dynamic loading*, Engineering Fracture Mechanics, 273, 108731.
40. Wang, P., Yuan, P., Sahmani, S., Safaei, B., 2021, *Surface stress size dependency in nonlinear free oscillations of FGM quasi-3D nanoplates having arbitrary shapes with variable thickness using IGA*, Thin-Walled Structures, 166, 108101.
41. Meschino, M., Wang, L., Xu, H., Moradi-Dastjerdi, R., Behdinan, K., 2021, *Low-frequency nanocomposite piezoelectric energy harvester with embedded zinc oxide nanowires*, Polymer Composites, 42(9), pp. 4573–4585.
42. Moradi-dastjerdi, R., Malek-Mohammadi, H., 2017, *Free vibration and buckling analyses of functionally graded nanocomposite plates reinforced by carbon nanotube*, Mechanics of Advanced Composite Structures, 4(1), pp. 59–73.
43. Safaei, B., Moradi-Dastjerdi, R., Qin, Z., Chu, F., 2019, *Frequency-dependent forced vibration analysis of nanocomposite sandwich plate under thermo-mechanical loads*, Composites Part B: Engineering, 161, pp. 44–54.
44. Sahmani, S., Safaei, B., Aldakheel, F., 2021, *Surface elastic-based nonlinear bending analysis of functionally graded nanoplates with variable thickness*, The European Physical Journal Plus, 136(6), pp. 1–28.
45. Qiu, J., Sahmani, S., Safaei, B., 2020, *On the NURBS-based isogeometric analysis for couple stress-based nonlinear instability of PFGM microplates*, Mechanics Based Design of Structures and Machines, pp. 1–25.
46. Lu, H., Zhou, J., Sahmani, S., Safaei, B., 2021, *Nonlinear stability of axially compressed couple stress-based composite micropanels reinforced with random checkerboard nanofillers*, Physica Scripta, 96(12), 125703.
47. Wang, J., Ma, B., Gao, J., Liu, H., Safaei, B., Sahmani, S., 2022, *Nonlinear stability characteristics of porous graded composite microplates including various microstructural-dependent strain gradient tensors*, International Journal of Applied Mechanics, 14(1), 2150129.
48. Sahmani, S., Safaei, B., 2020, *Influence of homogenization models on size-dependent nonlinear bending and postbuckling of bi-directional functionally graded micro/nano-beams*, Applied Mathematical Modelling, 82, pp. 336–358.
49. Yang, X., Sahmani, S., Safaei, B., 2021, *Postbuckling analysis of hydrostatic pressurized FGM microsized shells including strain gradient and stress-driven nonlocal effects*, Engineering with Computers, 37(2), pp. 1549–1564.
50. Liu, Y., Qin, Z., Chu, F., 2021, *Nonlinear forced vibrations of FGM sandwich cylindrical shells with porosities on an elastic substrate*, Nonlinear Dynamics, 104(2), pp. 1007–1021.
51. Li, H., Lv, H., Sun, H., Qin, Z., Xiong, J., Han, Q., Liu, J., Wang, X., 2021, *Nonlinear vibrations of fiber-reinforced composite cylindrical shells with bolt loosening boundary conditions*, Journal of Sound and Vibration, 496, 115935.

52. Liu, Y., Qin, Z., Chu, F., 2021, *Nonlinear forced vibrations of functionally graded piezoelectric cylindrical shells under electric-thermo-mechanical loads*, International Journal of Mechanical Sciences, 201, 106474.
53. Moradi-Dastjerdi, R., Behdinan, K., 2021, *Free vibration response of smart sandwich plates with porous CNT-reinforced and piezoelectric layers*, Applied Mathematical Modelling, 96, pp. 66–79.
54. Liu, Y., Qin, Z., Chu, F., 2021, *Nonlinear forced vibrations of FGM sandwich cylindrical shells with porosities on an elastic substrate*, Nonlinear Dynamics, 104(2), pp. 1007–1021.
55. Xie, B., Sahmani, S., Safaei, B., Xu, B., 2021, *Nonlinear secondary resonance of FG porous silicon nanobeams under periodic hard excitations based on surface elasticity theory*, Engineering with Computers, 37(2), pp. 1611–1634.
56. Sahmani, S., Safaei, B., 2019, *Nonlinear free vibrations of bi-directional functionally graded micro/nano-beams including nonlocal stress and microstructural strain gradient size effects*, Thin-Walled Structures, 140, pp. 342–356.
57. Fan, F., Sahmani, S., Safaei, B., 2021, *Isogeometric nonlinear oscillations of nonlocal strain gradient PFGM micro/nano-plates via NURBS-based formulation*, Composite Structures, 255, 112969.
58. Li, Q., Xie, B., Sahmani, S., Safaei, B., 2020, *Surface stress effect on the nonlinear free vibrations of functionally graded composite nanoshells in the presence of modal interaction*, Journal of the Brazilian Society of Mechanical Sciences and Engineering, 42(5), pp. 1–18.
59. Yuan, Y., Zhao, K., Han, Y., Sahmani, S., Safaei, B., 2020, *Nonlinear oscillations of composite conical microshells with in-plane heterogeneity based upon a couple stress-based shell model*, Thin-Walled Structures, 154, 106857.
60. Fan, F., Xu, Y., Sahmani, S., Safaei, B., 2020, *Modified couple stress-based geometrically nonlinear oscillations of porous functionally graded microplates using NURBS-based isogeometric approach*, Computer Methods in Applied Mechanics and Engineering, 372, 113400.
61. Yuan, Y., Zhao, X., Zhao, Y., Sahmani, S., Safaei, B., 2021, *Dynamic stability of nonlocal strain gradient FGM truncated conical microshells integrated with magnetostrictive facesheets resting on a nonlinear viscoelastic foundation*, Thin-Walled Structures, 159, 107249.
62. Masters, I.G., Evans, K.E., 1996, *Models for the elastic deformation of honeycombs*, Composite structures, 35(4), pp. 403–422.
63. Gibson, I.J., Ashby, M.F., 1982, *The mechanics of three-dimensional cellular materials*, Proceedings of the Royal Society of London. A. Mathematical and Physical Sciences, 382(1782), pp. 43–59.
64. Sorohan, Ş., Sandu, M., Sandu, A., Constantinescu, D.M., 2016, *Finite Element Models Used to Determine the Equivalent In-plane Properties of Honeycombs*, Materials Today: Proceedings, 3(4), pp. 1161–1166.